

Transfers from TLI to Lunar Frozen Orbits with Applications to NASA's CLPS & Artemis Programs

Anthony L. Genova¹

National Aeronautics and Space Administration, Moffett Field, CA, 94035, USA

Dylan Morrison-Fogel²

Axient, Moffett Field, CA, 94035, USA

Paul Levinson-Muth³

National Aeronautics and Space Administration, Moffett Field, CA, 94035, USA

This paper will focus on trajectory transfers from trans-lunar injection (TLI) to lunar frozen orbits with applications to NASA's Commercial Lunar Payload Services (CLPS) and Artemis Human Landing System (HLS) programs. For a CLPS application, the CS-3 mission is explored, which will deploy a communications relay satellite in lunar elliptical frozen orbit followed by landing a payload on the lunar farside during dawn. Given HLS will land a crew near the lunar south pole with lighting and timing requirements, the effect of varying the Earth-Moon transit duration to influence the approach direction upon landing will be explored.

I. Nomenclature

| | |
|-------------------|---|
| a | = semi-major axis |
| dt | = time step |
| e | = eccentricity |
| $ELFO$ | = elliptical lunar frozen orbit |
| $F_{Moon-Sun}$ | = Moon-Sun rotating frame |
| $HELO$ | = highly elliptical lunar orbit |
| i | = inclination |
| LEO | = low-earth orbit |
| LOI | = lunar orbit insertion |
| LLO | = low lunar orbit |
| MCI | = Moon-Centered Inertial reference frame |
| MCS | = Mission Control Sequence |
| $NRHO$ | = near-rectilinear halo orbit |
| $RAAN$ | = right ascension of the ascending node |
| $RAAN_{Moon-Sun}$ | = right ascension of the ascending node (Moon-Sun rotating frame) |
| TOD | = true-of-date frame |
| TLI | = trans-lunar injection |
| ΔV | = change in velocity |
| ω | = argument of periapsis |
| v | = true anomaly |

¹ Astrodynamics Subject Matter Expert, Spaceflight Division, Ames Research Center, AIAA Member

² Flight Dynamics Analyst, Axient, Spaceflight Division, Ames Research Center, AIAA Member

³ Flight Systems Engineer, Spaceflight Division, Ames Research Center, AIAA Member

II. Introduction

The trajectories presented in this paper are applied to both NASA’s Commercial Lunar Payload Services (*CLPS*) and *Artemis* programs, including the Human Landing System (*HLS*), which target near-term exploration of cislunar space and the lunar surface. The *CLPS* program will execute lunar missions to support *HLS* and has already funded multiple U.S. commercial companies to land payloads on the lunar surface, specifically on the lunar farside, south polar region, and other regions of scientific interest [1]. Meanwhile, NASA’s *HLS* program has selected *SpaceX* and *Blue Origin* as to fly a series of *Artemis* missions that will land crew near the lunar south pole [2-4]. Furthermore, the results in this paper map to several objectives listed in the *National Cislunar Science and Technology Strategy* published by the Office of Science and Technology Policy within the White House Executive Office of the President [5].

Given that both *CLPS* and *HLS* will target the lunar south pole region with constrained timing and lighting requirements before the end of this decade, there is overlap regarding their trajectory designs. To help evaluate such trajectories, the *Lunar Browser* tool has been in development, which uses *Python* to “drive” *STK/Astrogator* and populate the cislunar solution space assuming a launch from Kennedy Space Center (KSC), insertion to low-Earth orbit (LEO), followed by trans-lunar injection (TLI) with varying coast durations to the Moon computed to allow for lunar orbit insertion (LOI) performed above the north and south poles of the Moon for entry into lunar polar orbit. *Lunar Browser* can filter the global solution database for specific trajectories with complex logic control according to mission needs. Results considered for *CLPS* and *Artemis* scenarios are presented herein.

III. Software Tools, Assumptions, & Constraints

The primary software tool used for the presented trajectory analysis was *STK/Astrogator*, which utilized an 8th/9th order Runge-Kutta numerical integrator for orbit propagation within a force model that included an N-body gravity field (50X50 Earth and Moon gravity fields and point masses for all other planets), thermal and solar radiation pressure, and atmosphere models at Earth (Jacchia-Roberts), unless otherwise specified. Other software analysis tools used included: NASA’s *Lunar Browser* (a tool still in the development phase), which drives *STK/Astrogator* via *Python*, to generate a large database of Earth-Moon trajectory transfers. The methodology used for this solution generation is described in the next section.

IV. Lunar Transfer Search Strategies

We adopted several strategies for building a database of Earth-Moon transfers via the *Lunar Browser* tool currently under development and not publicly available. Initially, we wrote a simple and consistent direct lunar transfer sequence in *STK/Astrogator*’s Mission Control Sequence (MCS): launch from KSC, coast in a circular 185 km LEO, TLI in the velocity direction, coast to perilune at 100 km altitude, and LOI to circularize to low lunar orbit (LLO). While some aspects of this sequence may require tailoring to meet a given mission’s capabilities (e.g., dividing LOI across multiple passes, targeting alternative altitudes), the use of a simple and consistent transfer sequence provides the advantages of enabling direct comparison between candidate transfers, use of previous results as initial conditions for further searches, and easy identification of families and trends in the solution set.

A. Filling in the Lunar Transfer Database

We populated families of direct lunar transfers by incrementing one or more elements of previous solutions’ initial conditions and retargeting the adjusted solutions using a differential corrector and high-fidelity force model in *STK/Astrogator*. Certain sets of initial conditions failed to converge to a viable transfer, and plots of previous solutions served as useful tools for identifying regions of the search space where new solutions might exist. Plots of coast duration vs. launch epoch proved especially useful for identifying patterns in the solution set. When viewed in a coast duration vs. launch epoch plot, direct transfer solutions typically fall into “families” of coast durations, with each family spanning a range of coast durations equal to half the orbit period of the LEO coast orbit. For example, Fig. 1 shows solutions falling into 3 families, with the families’ upper-bound coast durations at approximately 35 minutes, 80 minutes, and 125 minutes.

Plots of previous solutions also enabled identification of regions of the search space unlikely to result in successful transfers. For example, Fig. 1 includes recurring discontinuities between groups of successful solutions. Discontinuities in the solution sets typically occur at boundaries between some families – as coast durations approach the 35-minute boundary between the first two families, we see gaps in each family spanning ~3 days along the “Launch

Epoch” axis. The boundaries of these gaps appear to vary as a function of the duration of the lunar approach, labeled “Duration TLI-LOI” in the figure. Such gaps do not occur at the 80-minute boundary, but we begin to see evidence of discontinuities near the 125-minute boundary. Identification of recurring discontinuities helps streamline the process of populating transfer solutions by focusing the effort on viable regions of the search space. The discontinuities in the coast duration vs. launch epoch plots divide the families of solutions into groups, with each group spanning a lunar cycle of launch opportunities and half an orbit cycle of coast duration.

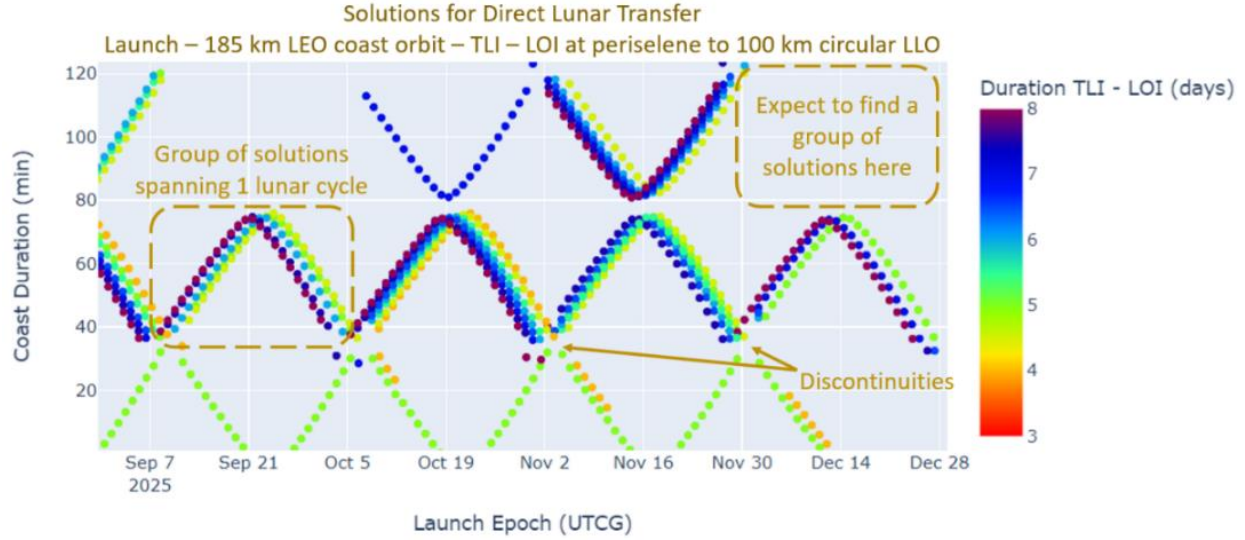


Fig. 1. Coast duration vs. launch epoch for a set of direct transfer solutions, with time of flight from TLI to LOI indicated by the color bar.

B. Searching for Solutions with Adjusted TLI-LOI Time of Flight

We can typically use a solution within a group to serve as an initial condition when searching for other solutions within that group. For example, if we have found solutions with TLI-LOI coast durations of 5 days within a given group, we can use those solutions as initial conditions to search for solutions with 3-day TLI-LOI coast durations, as shown in Fig. 2. In this case, we would use the following workflow to generate each new solution: (1) identify the existing solution to use as an initial guess, (2) apply the previous solution’s maneuver magnitudes and launch epoch as initial conditions but change the desired TLI-LOI duration to 3 days, (3) use a differential corrector in *STK/Astrogator* to target each new solution, and (4) save the new solution if the differential corrector converged. By using a script to iterate over this workflow, we can generate solutions spanning a large set of desired TLI-LOI durations.

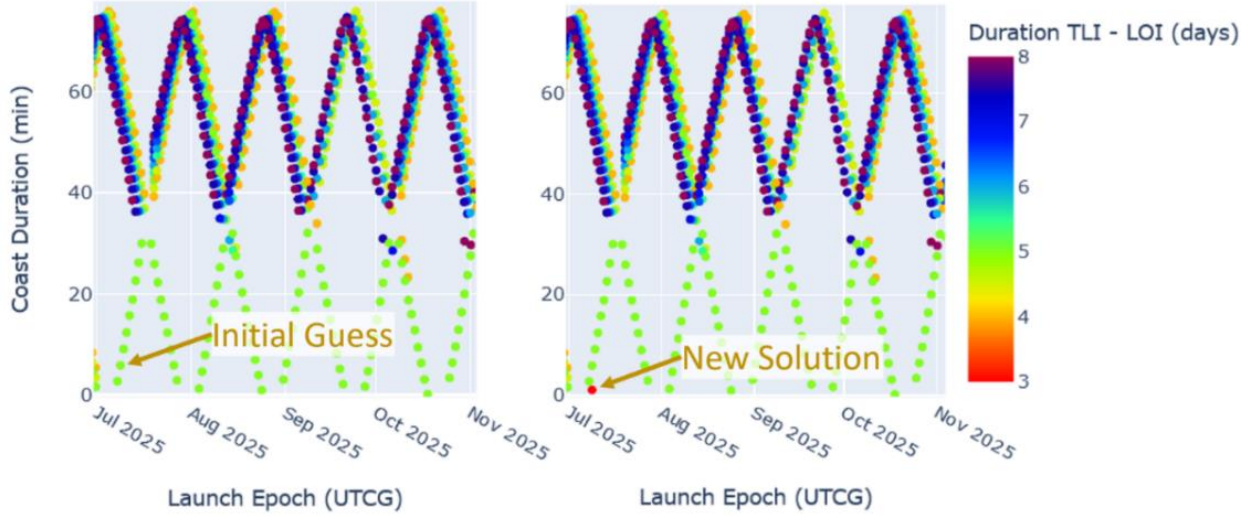


Fig. 2. A solution with a 5-day TLI-LOI time of flight serves as an initial guess to find a solution with a 3-day TLI-LOI time of flight.

C. Filling in Solutions with the Same TLI-LOI Time of Flight

Similarly, if we have a single 5-day TLI-LOI solution within a group, we can use that solution as an initial condition to search for additional 5-day TLI-LOI solutions (Fig. 3). In this case, the workflow for generating each new solution would increment each initial launch epoch by approximately 1 day while keeping the desired TLI-LOI duration fixed; the rest of the workflow would remain unchanged, utilizing a differential corrector to target new solutions and saving each converged result. Solutions within a group tend to have launch epochs offset by approximately 1 day from each previous solution, so 1-day increments tend to result in differential corrector convergence. As in the previous example, using a script to iterate over this workflow enables timely generation of large solution sets.

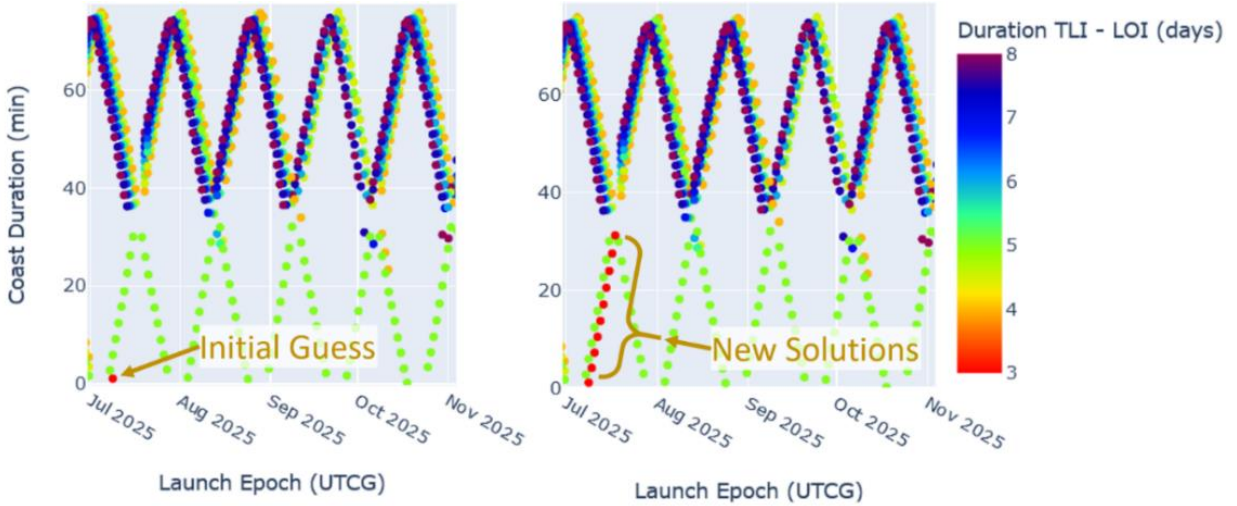


Fig. 3. A solution with a 3-day TLI-LOI time of flight serves as an initial guess to find additional solutions with 3-day TLI-LOI times of flight.

D. Searching for Solutions Spanning Multiple Lunar Cycles

As previously noted, solutions tend to form groups spanning 1 lunar cycle, with gaps of ~ 3 days between each group. While we can fill in solutions spanning a lunar cycle by selecting an initial guess within the cycle and iteratively searching over 1-day launch epoch increments, we also need strategies to search for solutions in subsequent lunar cycles. To generate solutions in previously unsearched lunar cycles, we can use 27- or 28-day launch epoch increments – these increments correspond to approximately 1 lunar cycle. Figure 4 shows an example, with 28-day time increments generating 9 solutions from an initial guess. Note that switching the increment between 27 and 28 days generally changes the coast duration trend in the newly generated solutions – in the example shown, the 28-day increment leads each solution to have a shorter coast duration than the previous solution, and a 27-day increment would lead each solution to have a longer coast duration than the previous. Alternating 27- and 28-day increments can enable iterative searches spanning many lunar cycles within a single family of coast durations.

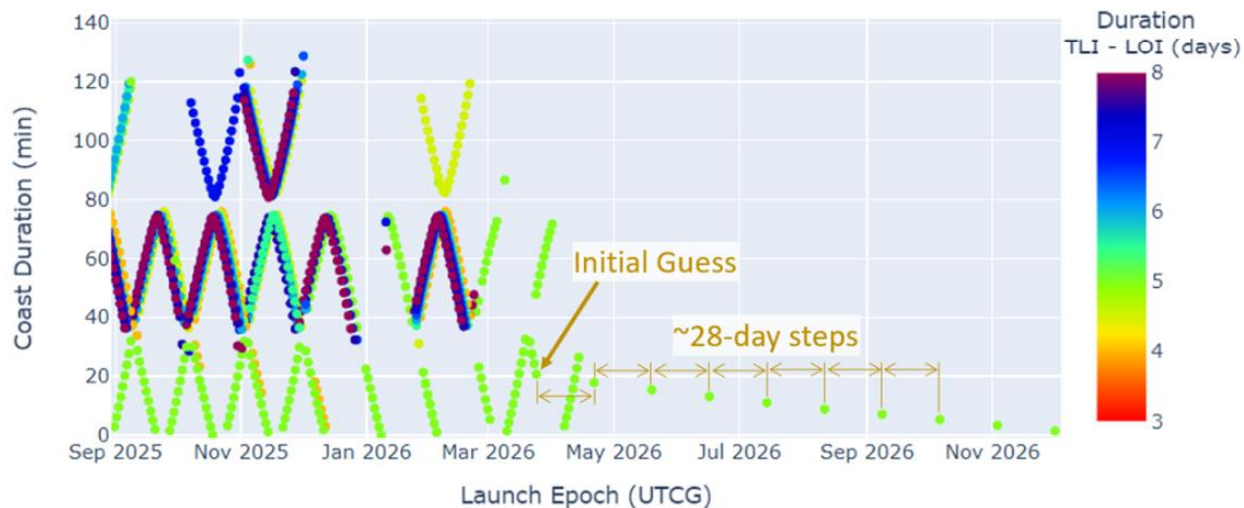


Fig. 4. Time increments of 27 or 28 days allow the *STK/Astrogator* Command Window to find lunar transfer solutions spanning multiple lunar cycles.

V. Trajectory Design with Application to NASA’s CLPS Program

While the *Lunar Browser* tool can apply to multiple *CLPS* missions, this section focuses on applications to the relatively complex *CLPS* mission: *CS-3*. This mission will plan to launch from NASA KSC with a lunar lander to be provided by *FireFly Aerospace* which hosts the *LuSEE-Night* payload both of which are attached to a communications relay satellite *Lunar Pathfinder* provided by the European Space Agency [6].

After coasting in LEO and performing the TLI, the system will coast in cislunar space with a lunar encounter 4-8 days later. Near perilune, the LOI will be performed above the lunar north pole which will insert all spacecraft into an elliptical frozen lunar orbit (ELFO) with apsides near 90 degrees; in this orbit, *Lunar Pathfinder* will be deployed. The lunar lander and *LuSEE-Night* will later descend to low lunar orbit (LLO), assumed to have 100 km altitude and 90-degree inclination, followed by a coast period in LLO to allow for alignment with the lunar farside landing site during dawn. Although the nominal science operations will occur during daylight on the first lunar day following landing, the *LuSEE-Night* payload (a collaboration between NASA’s Science Mission Directorate, Department of Energy’s Brookhaven National Laboratory, and the University of California, Berkeley, Space Sciences Laboratory) will continue to operate during lunar nights to observe Dark Ages sensitive radio waves for the first time [6,7]. Although exact mission parameters and requirements are not specified, the general trajectory design presented serves as a proof-of-concept for *CS-3* and a guide to recognize trends relevant to deploying a spacecraft in an ELFO followed by a dawn landing at a lunar farside site, without the need for changing the orbital plane after LOI. The specific ELFO inclination and argument of perilune, ω , of 90 degrees utilized are in/near the family of frozen orbits studied previously by Ely [8] with the full list of orbital elements, along with other assumptions, constraints, and requirements related to the trajectory design, seen in Table 1.

The MCS is written in *STK/Astrogator* which corresponds to a proof-of-concept trajectory for *CS-3*’s lander trajectory from launch to the LLO immediately preceding the landing/descent sequence with view in the Moon-centered inertial (MCI) reference frame (Fig. 5). The lander separates from the communications relay satellite before

the “DRIFT COAST” phase with 3 m/s relative velocity, which can be varied slightly to ensure line-of-sight between the relay satellite and the lander (and between the relay satellite and Earth) during the descent sequence. The communications relay satellite propagates after this separation without the need for deterministic maneuvers. The descent sequence is designed in a separate MCS which ensures a co-planar transfer from LLO to landing (i.e., for the LLO to pass directly above the surface site at/near dawn) by slightly adjusting the altitude of the LLO to iteratively solve the end-to-end trajectory.

Table 1. Assumptions, Constraints, and/or Requirements for CLPS CS-3 Trajectory Design

| Category | Assumption, Constraint, and/or Requirement |
|---|---|
| Launch analysis nominal timeframe | Oct. 25, 2025 to Jan. 25, 2026 |
| Launch site | NASA Kennedy Space Center |
| Transfer duration from TLI to LOI | 4 to 8 days |
| Solar eclipse maximum duration from TLI to LOI | 2 hours |
| Maneuver modeling | Orbiter uses high thrust-to-mass ratio and impulsive maneuvers within <i>STK/Astrogator</i> ; transfers are co-planar after LOI |
| ELFO parameters | $i = 56.2$ deg. (posigrade cases) & 123.8 deg. (retrograde cases), $\omega = 90$ deg., Altitudes: perilune = 750 km, apolune = 7,500 km |
| Lunar farside site location & elevation angle constraint for communications to orbiting relay | Latitude near -20 degrees, Longitude near 180 degrees with 25-degree elevation angle constraint for communications |
| Timing & lighting constraints of lunar landing | During dawn (i.e., within 2 Earth days of sunrise at surface site) |
| LLO parameters | 100 km circular ($e = 0$) and $i = 56.2$ deg (posigrade cases) or $i = 123.8$ deg (retrograde cases) |
| Maximum LLO loiter duration prior to landing | 28 days |

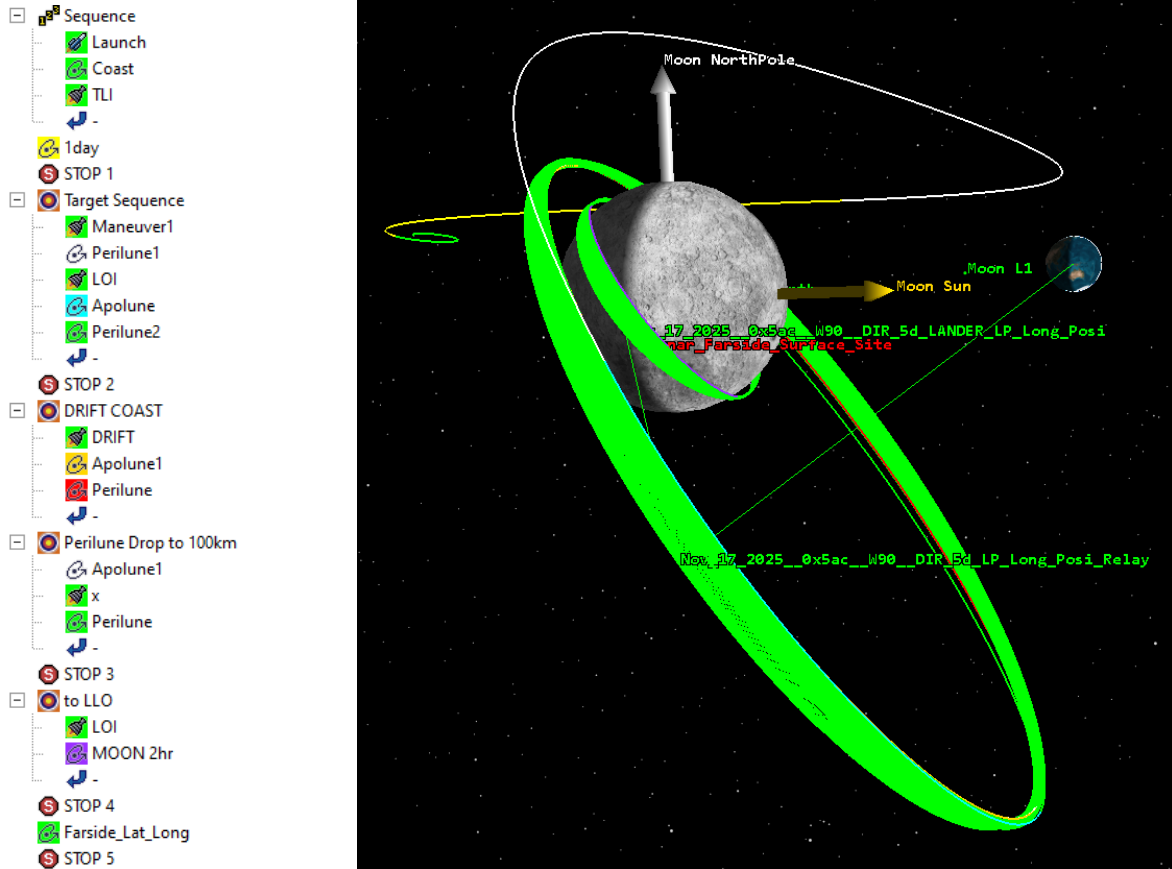


Fig. 5. CLPS CS-3 proof-of-concept trajectory solved in *STK/Astrogator* with MCS displayed (left) and trajectory visualized in the Moon inertial reference frame (right).

Given the lighting constraint of the lander needing to touch down at the specified lunar farside site during dawn, the RAAN at LOI was specifically analyzed in the Moon-Sun rotating frame, ($\mathcal{F}_{Moon-Sun}$). To define this frame, we adopt the convention of the x-axis aligning with the Moon-Sun vector, the z-axis aligning with the Moon's angular momentum about the Sun, and the y-axis completing the right-handed system. We define the $RAAN_{Moon-Sun}$ angle as the dihedral angle from the $\mathcal{F}_{Moon-Sun}$ x-axis to the ascending node of a lunar orbit, measured about the $\mathcal{F}_{Moon-Sun}$ z-axis (Fig. 6). It's important to note that the rotation of $\mathcal{F}_{Moon-Sun}$ causes $RAAN_{Moon-Sun}$ to behave differently from the familiar RAAN (i.e., RAAN measured in an inertial frame) – as the Earth-Moon system orbits the Sun, the $RAAN_{Moon-Sun}$ of a given lunar orbit decreases in value (i.e., $dRAAN_{Moon-Sun}/dt < 0$). The value of $RAAN_{Moon-Sun}$ measured at a selected epoch provides information about solar access at that epoch. It is noted that $RAAN_{Moon-Sun}$ values of ~ 90 and ~ 270 degrees in LLO yield landings to the assumed CS-3 site at lunar dawn, which could provide ~ 14 Earth days of sunlight before lunar dusk. However, it is not yet known as to what values of $RAAN_{Moon-Sun}$ at the time of LOI correspond to such RAAN values prior to landing.

Daily sampling of trajectories from launch to LLO was performed with the purpose of identifying a pattern with respect to the $RAAN_{Moon-Sun}$ at the time of LOI. Such a pattern did emerge for both posigrade and retrograde inclination assumptions for the ELFO; values of **~ 120 , ~ 270 , and ~ 300 degrees** were observed at LOI (from the *Lunar Browser* results) which yielded co-planar transfers to LLO followed by alignment with the specified farside site to set up a dawn landing.

The *Lunar Browser* Filter function and Logic Control were then used to identify transfer solutions within 10 degrees of each identified $RAAN_{Moon-Sun}$ to identify candidate CS-3 trajectory solutions with nominal launch dates between Oct. 25, 2025 and Jan. 25, 2026. The *Lunar Browser* results are plotted in Fig. 7 which shows monthly opportunities for the three viable ranges of $RAAN_{Moon-Sun}$ values near of **~ 120 , ~ 270 , and ~ 300 degrees**.

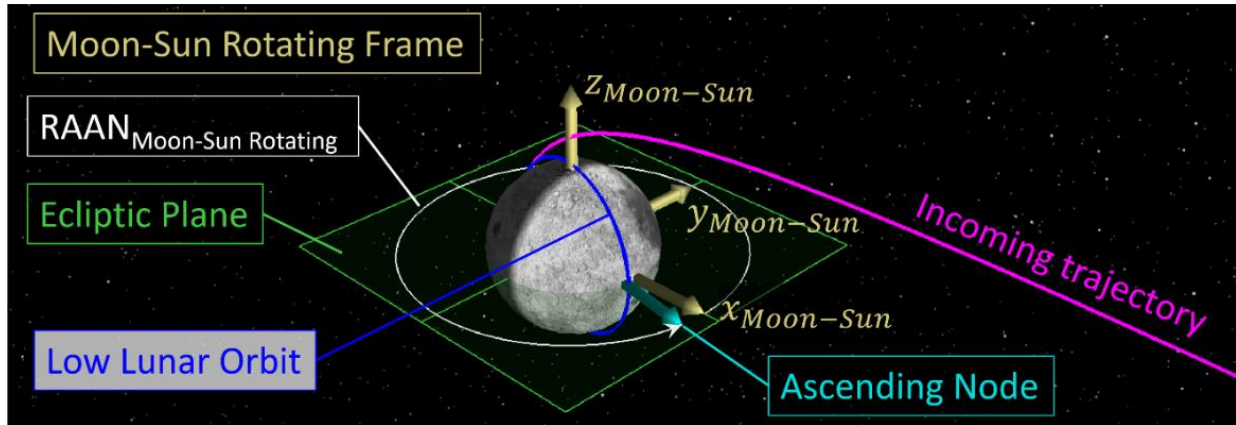


Fig. 6. Diagram illustrating the $RAAN_{Moon-Sun}$ angle. In the example shown, the $RAAN_{Moon-Sun}$ angle (measured at the epoch of lunar orbit insertion) is 351 degrees.

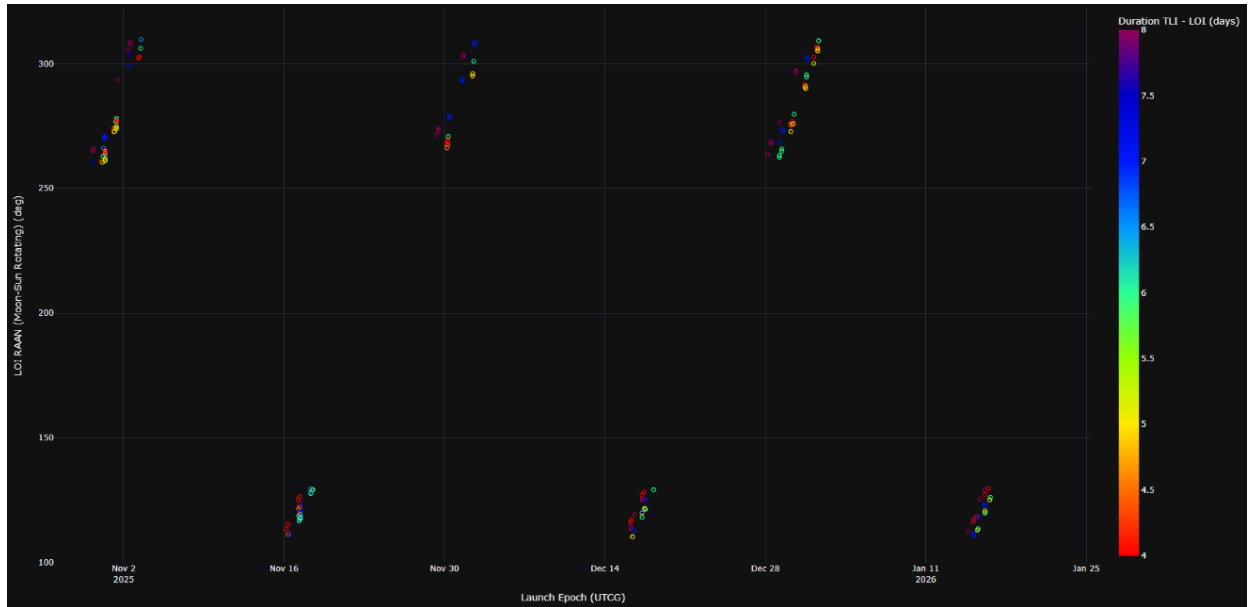


Fig. 7. Earth-Moon transfer trajectories filtered to show candidate trajectory solutions for CS-3 with RAAN(Moon-Sun) values near ~120, ~270, and ~300 degrees throughout a launch timeframe of Oct. 25, 2025 to Jan. 25, 2026.

For solution families deploying a relay satellite with posigrade inclination in an ELFO and $RAAN_{Moon-Sun}$ value of ~120 degrees at LOI, the family is categorized as a “posigrade northwest solution family” given its descending motion from the northwest direction upon landing at the selected farside site. The “posigrade southwest solution family” also deploys the relay satellite with posigrade inclination yet approaches the farside site with ascending motion from the southwest ($RAAN_{Moon-Sun}$ ~300 degrees); both families are displayed in Fig. 8.

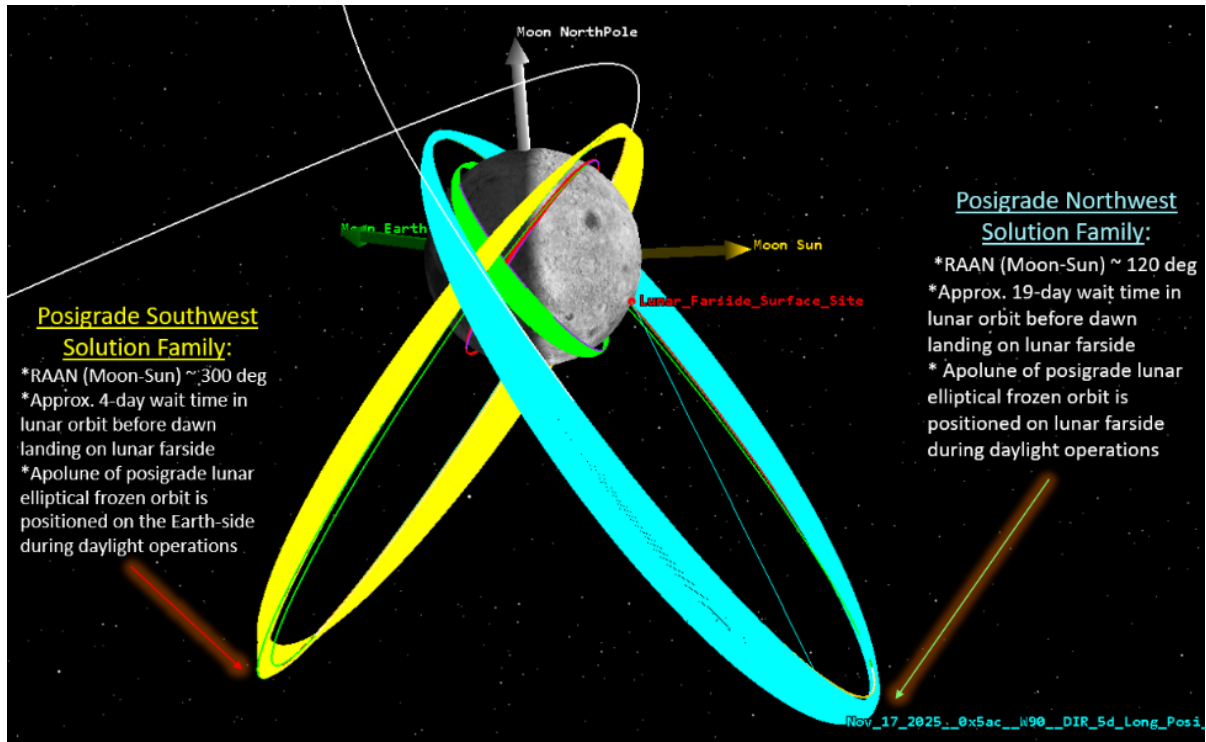


Fig. 8. Both Posigrade Northwest and Southwest solution families allow a drop-off of the communications relay satellite in required ELFO (posigrade inclination).

There are also solution families that deploy the communications relay satellite in ELFO with retrograde inclination, which provides another option with relatively low loiter duration in LLO (i.e., 7 days) with apolune of the ELFO located on the farside of the Moon (e.g., at solar noon following landing). The retrograde descending family is termed “retrograde northeast” as it approaches the landing site from the northeast while the retrograde ascending family is specified as “retrograde southeast” as it approaches from the southeast. Examples of both retrograde northeast and southeast solution families are seen in Fig. 9. Also note that both retrograde families yield an approach over sunlit terrain during descent which may help enable a safe landing (e.g., by improving terrain relative navigation).

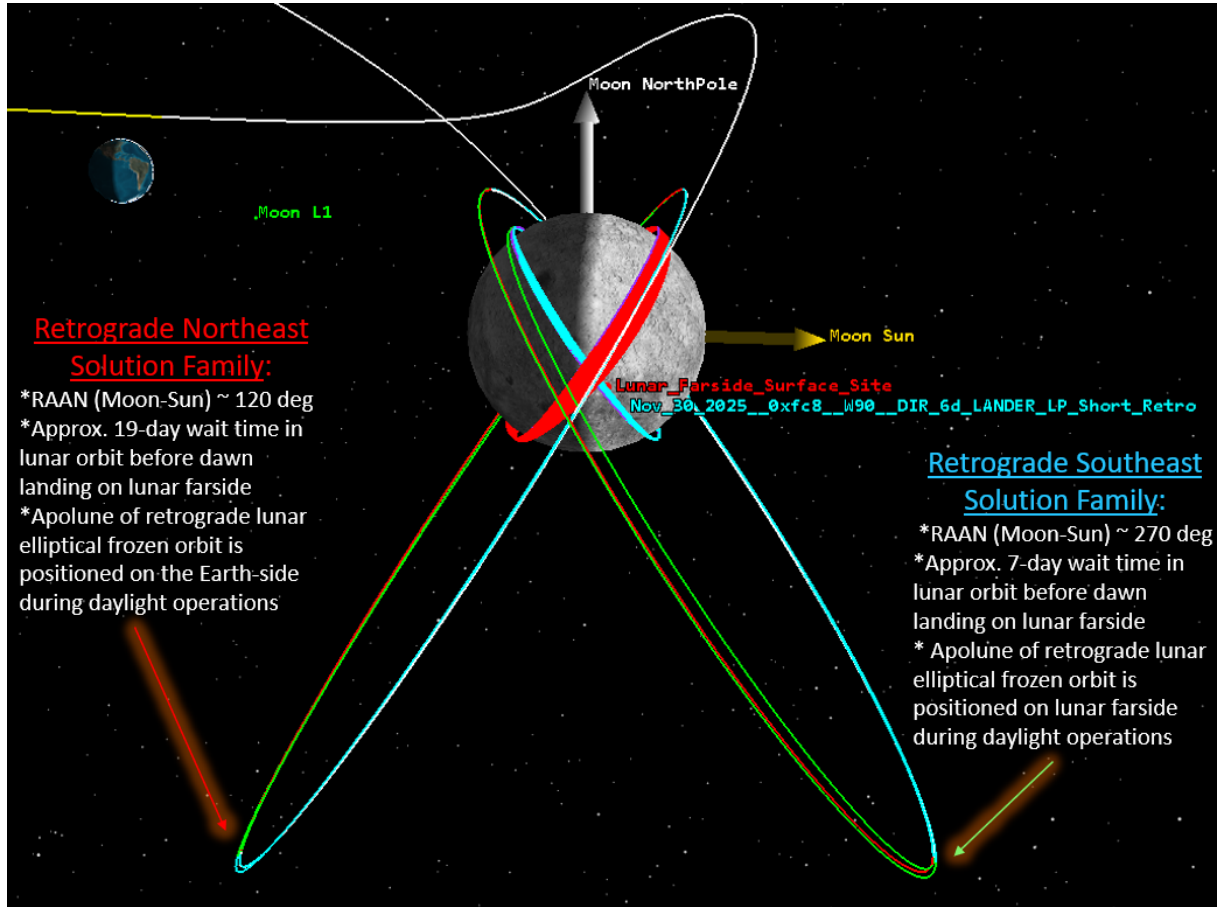


Fig. 9. Both Retrograde Northeast and Southeast family solutions allow a drop-off of the communications relay satellite in required ELFO (retrograde inclination).

All four solution families are color-coded and compiled in Table 2. It is seen that 2 families with apolune of the ELFO located on the lunar farside at solar noon following landing yield significantly more cumulative hours (i.e., >150 hours vs. ~30 hours) between a deployed relay satellite and the selected lunar farside site: 1) posigrade northwest and 2) retrograde southeast. Given the lower loiter duration requirement in LLO of approximately 7 days among these 2 families, the **retrograde southeast family** (green color-code in Table 2) is considered the most favorable. Further details are seen with respect to this family after extending solutions forward to include launch epochs through Jan. 2027. The time spent from TLI to LOI is seen to range from 4 to 8 days (integer values only were considered), while the time spent in LLO until landing includes a range from 4.14 to 9.46 days (Fig. 10). Also, in Fig. 10, the time spent from TLI to landing is seen to range from 10.79 to 13.72 days. While not every launch epoch is visible on Fig. 10, it was observed that solutions for this family exist for up to three consecutive launch days spaced approximately one month apart. Implementation of Earth phasing orbits is one method of expanding this 3-day monthly launch period.

For both southern families (*posigrade southwest* and *retrograde southeast*) $RAAN_{Moon-Sun}$ values in the range of ~255 to ~285 degrees were observed with ~255 degrees at landing ensuring the local time is dawn at the selected farside site. For both northern families (*posigrade northwest* and *retrograde northeast*), $RAAN_{Moon-Sun}$ values in the range of ~75 to ~105 degrees were observed. Future work may explore varying the time spent in different Earth and lunar orbits such that $dRAAN_{Moon-Sun}/dt$ from TLI to landing yields a touchdown with the surface at dawn.

Table 2. Candidate Trajectories from *Lunar Browser* extended in *STK/Astrogator* to construct end-to-end CS-3 Solutions with 4 Families Shown (distinct families highlighted with matching colors) that include Posigrade and Retrograde inclinations for ELFO, with launch between October 25, 2025 & January 25, 2026.

| Trajectory # | Launch Date | Solution Family Name | RAAN (Moon-Sun) at LOI (deg) | Time from TLI to LOI (days) | Time in LLO prior to landing (days) | Epoch of Lunar Landing at Farside Site (UTCG) | Time from sunrise to landing (hrs) | Cumulative Contact Hours (Relay to Farside Site) | ΔV to Deploy Relay in ELFO (m/s) | Total Deterministic ΔV for Lander (m/s) |
|--------------|---------------|----------------------|------------------------------|-----------------------------|-------------------------------------|---|------------------------------------|--|--|---|
| 1 | Oct. 31, 2025 | Retrograde Southeast | 261.1 | 5 | 6.7 | 13 Nov 2025 12:45:50.862 | ~17 | ~156 | ~546 | ~2,790 |
| 2 | Nov. 1, 2025 | Posigrade Southwest | 293.4 | 8 | 1.9 | 12 Nov 2025 20:57:38.800 | ~1 | ~35 | ~573 | ~2,817 |
| 3 | Nov. 17, 2025 | Posigrade Northwest | 119.3 | 5 | 19.1 | 12 Dec 2025 21:34:57.145 | ~11 | ~157 | ~506 | ~2,750 |
| 4 | Nov. 17, 2025 | Retrograde Northeast | 119.3 | 5 | 19 | 12 Dec 2025 23:17:13.087 | ~13 | ~27 | ~507 | ~2,751 |
| 5 | Nov. 30, 2025 | Retrograde Southeast | 270.7 | 6 | 6.7 | 13 Dec 2025 13:35:42.308 | ~27 | ~154 | ~547 | ~2,791 |
| 6 | Dec. 1, 2025 | Posigrade Southwest | 293.9 | 7 | 2.8 | 12 Dec 2025 19:07:19.301 | ~8.5 | ~32 | ~538 | ~2,782 |
| 7 | Dec. 17, 2025 | Posigrade Northwest | 120 | 5 | 19 | 11 Jan 2026 12:28:44.488 | ~11 | ~157 | ~510 | ~2,754 |
| 8 | Dec. 17, 2025 | Retrograde Northeast | 119.9 | 5 | 19 | 11 Jan 2026 18:11:00.017 | ~17 | ~26 | ~510 | ~2,754 |
| 9 | Dec. 30, 2025 | Retrograde Southeast | 272.8 | 5 | 6.5 | 12 Jan 2026 05:24:22.904 | ~28 | ~152 | ~516 | ~2,760 |
| 10 | Jan. 1, 2026 | Posigrade Southwest | 305 | 5 | 4.4 | 12 Jan 2026 08:25:38.136 | ~33 | ~28 | ~487 | ~2,731 |
| 11 | Jan. 16, 2026 | Posigrade Northwest | 120 | 5 | 18.5 | 10 Feb 2026 01:22:30.743 | ~11 | ~157 | ~523 | ~2,767 |
| 12 | Jan. 16, 2026 | Retrograde Northeast | 120 | 5 | 19 | 10 Feb 2026 10:09:01.139 | ~20 | ~26 | ~542 | ~2,786 |

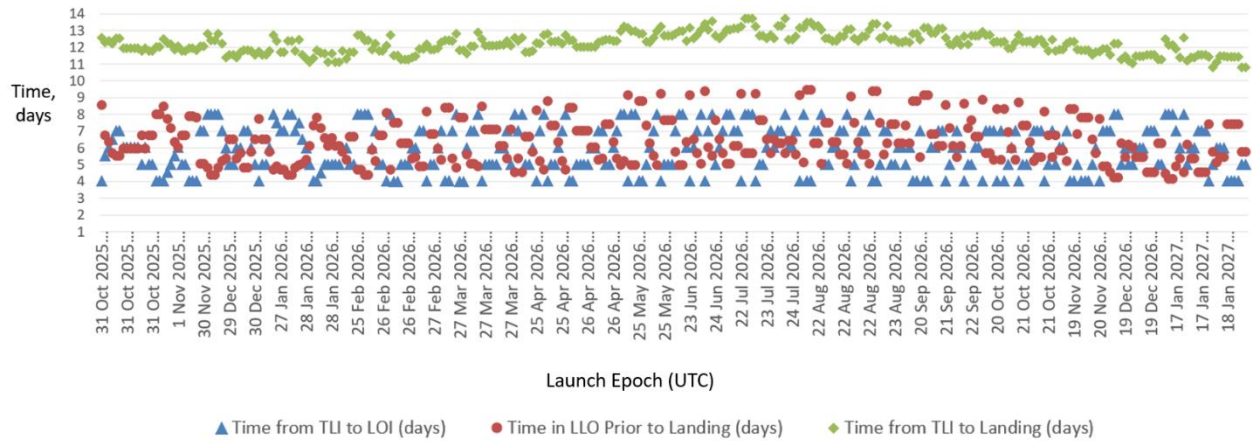


Fig. 10. Retrograde Southeast family solutions populated forward in time to include launch epochs through January of 2027, with Time spent from TLI to LOI, in LLO prior to landing, and from TLI to Landing plotted vs. Launch Epoch.

To check for long-term stability of the ELFOs for the most favorable solution family (i.e., **retrograde southeast family**) presented in Table 2, propagation was performed over a 5-year period using a 8th/9th order Runge-Kutta numerical integrator and high-fidelity gravity model in *STK/Astrogator*. As seen in Fig. 11, both lunar eccentricity (radial axis) and argument of perilune (angular axis) of the ELFOs are bounded over the 5-year timeframe for *Trajectories #1, #5, and #9* (Retrograde Southeast family), with the perilune altitude of the ELFOs for these three trajectories remaining above 200 km as seen in Fig. 12.

Future work may expand the solution space for all four families presented, perform long-term propagation of these solutions, and assess relative orbit stability (i.e., orbit plane separation of constellations over time).

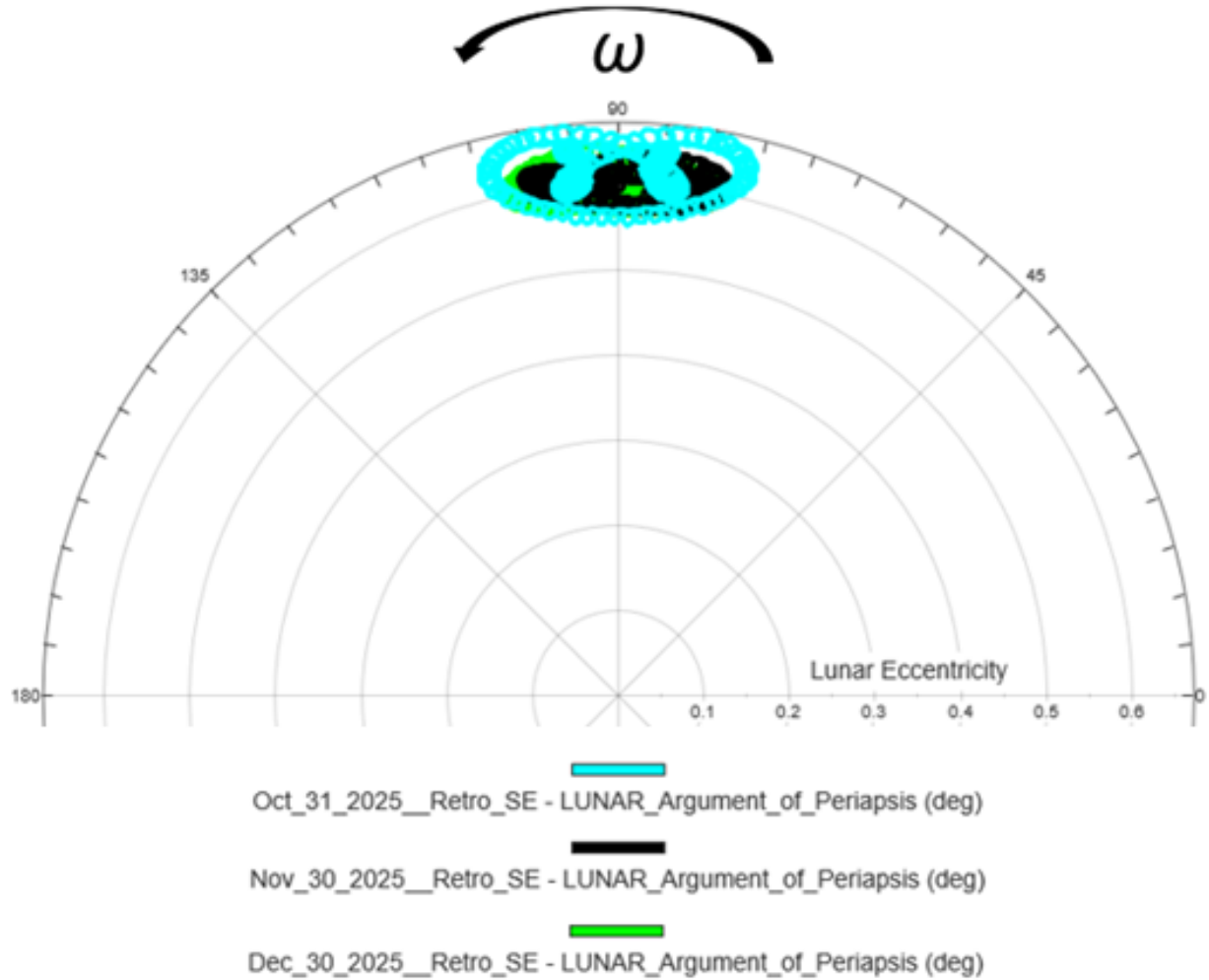


Fig. 11. Polar Plot of eccentricity (radial axis) and argument of perilune (angular axis) assuming 5 years of orbit propagation for the ELFOs corresponding to Trajectories #1, #5, and #9 (i.e., Retrograde Southeast Families) from Table 2.

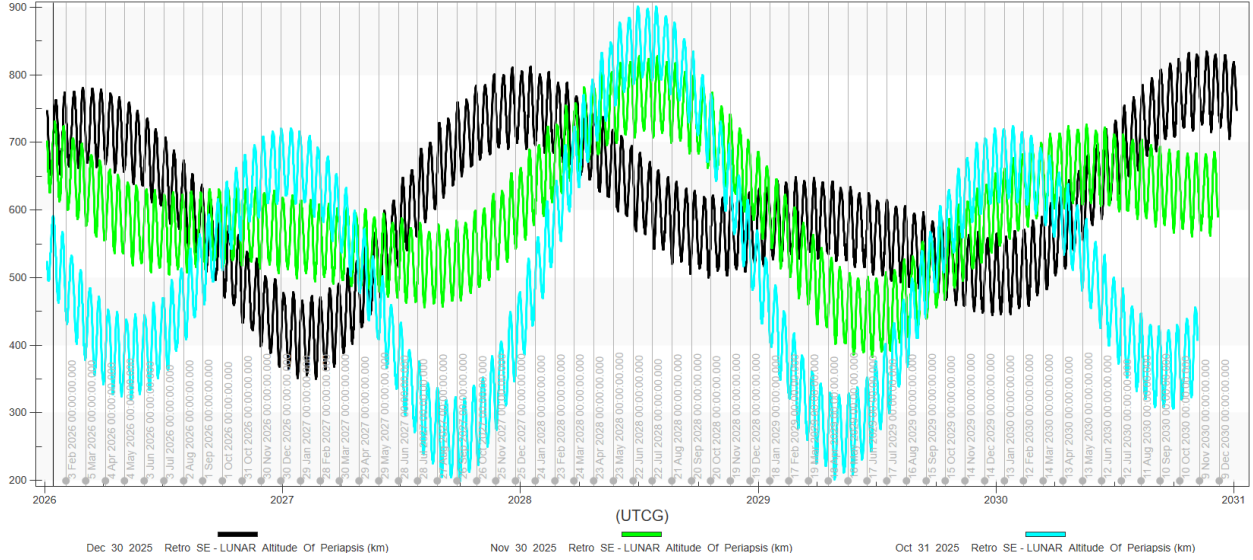


Fig. 12. Perilune Altitude of ELFOs for Trajectories #1, #5, and #9 (Retrograde Southeast Family) plotted vs. time over 5-year period.

VI. Trajectory Design with Application to NASA's Artemis Program

NASA's *Artemis* program plans to fly a series of lunar missions which will land crew on the lunar surface for the first time since the *Apollo* program. The first crewed landing mission will be *Artemis III* which will target the lunar south pole region for its landing site [9] no earlier than December 2025 according to the *Artemis* schedule listed in NASA's FY24 Budget Request [10]. Given the transfer trajectories generated by *Lunar Browser* target a polar LLO, there are applications to *Artemis* with respect to the approach direction at LOI, which is directly related to $RAAN_{Moon-Sun}$. This application will be explored in the next section using assumptions, constraints, and requirements listed in Table 3. An additional application presented in the final section explores a lunar frozen orbit near the assumed 100 km polar circular LLO.

Table 3. Assumptions, Constraints, and/or Requirements for Artemis & HLS Trajectory Design

| Category | Assumption, Constraint, and/or Requirement |
|---|---|
| Launch analysis nominal timeframe | December 1, 2025 to March 31, 2026 |
| Launch site | NASA Kennedy Space Center |
| Outbound transit duration from TLI to LOI | 4 to 12 days |
| Maneuver modeling | Orbiter uses high thrust-to-mass ratio and impulsive maneuvers within <i>STK/Astrogator</i> |
| Pre-Descent LLO parameters | 100 km circular ($e = 0$) and polar ($i = 90$ degrees) |

A. Effect of Varying Outbound Transit Duration on $RAAN_{Moon-Sun}$ at LOI

There is importance in selecting a viable approach angle (and thus $RAAN_{Moon-Sun}$) for the *Artemis* crew as they descend to the lunar landing site at a particular epoch. The reasoning for this is that terrain relative navigation over sunlit terrain is critical for fine-tuning the exact landing location (e.g., to avoid unforeseen hazards) and avoiding flying over certain regions that may interfere with science operations in process near the south pole. Furthermore, there is value in considering alternate phased near-rectilinear halo orbits (NRHOs) and/or highly elliptical lunar orbits *HELOs* with similar properties, which would allow more flexibility with respect to the approach angle upon landing (expressed as $RAAN_{Moon-Sun}$) and thus increase overall mission and site availability [11]. This section explores the effect of varying the outbound transit duration, from TLI to LOI, on the $RAAN_{Moon-Sun}$ at LOI which can be applied to a mission profile containing alternate phased NRHOs or *HELOs*.

Given a range of 4 to 12 days for the outbound transit duration from TLI to LOI, it is seen in Fig. 13 that a 360-degree range of $RAAN_{Moon-Sun}$ is cycled through approximately every month for each value of transit duration. The LOI is performed above the lunar north pole which is also the case for insertion into the baseline NRHO.

Focusing on a smaller timeframe it is seen that for each launch day (i.e., 24-hour timespan), a ~ 50 -degree range of $RAAN_{Moon-Sun}$ is possible if the outbound transit duration can be selected between 4 and 12 days (Figs. 14 & 15). The trajectory profiles for a selected launch day in this window are displayed in the Earth-centered inertial (ECI) frame in Fig. 14 (left), where it is seen that apogee of the transfer trajectory gradually passes beyond lunar distance as the transit duration is increased. The corresponding ~ 50 -degree range of $RAAN_{Moon-Sun}$ at LOI (Fig. 15) is also seen in Fig. 14 (right) in the Moon-Sun rotating frame.

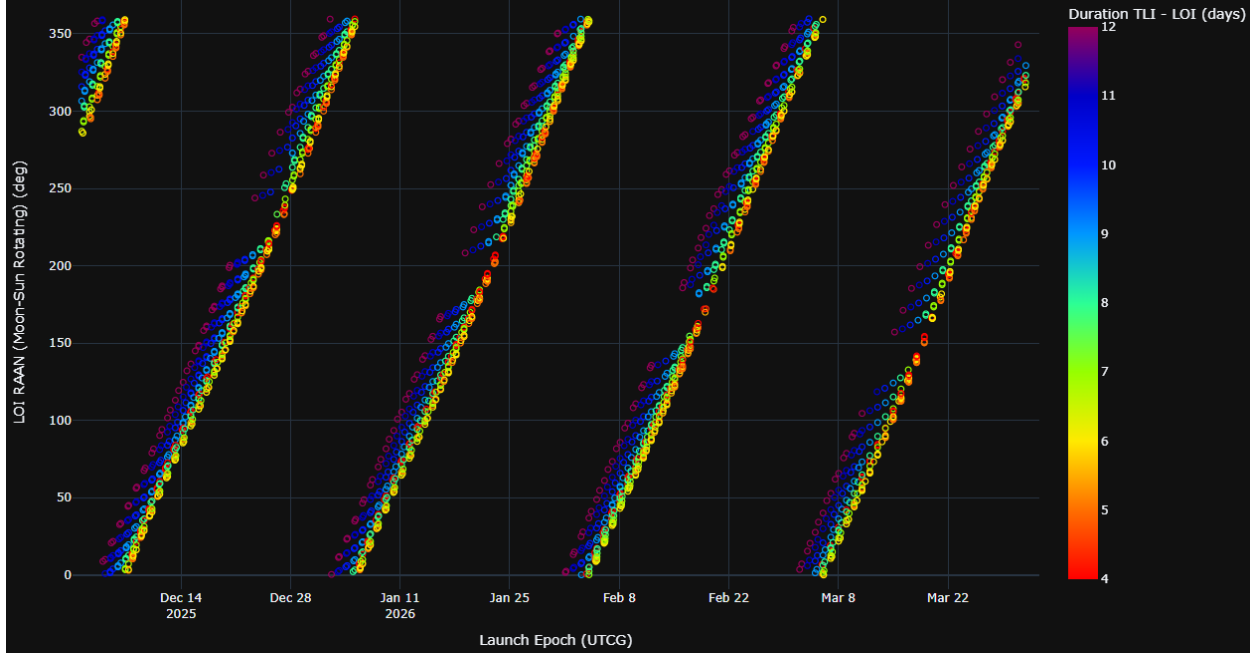


Fig. 13. TLI to LOI transit duration range from 4 to 12 days with $RAAN_{Moon-Sun}$ plotted for multiple launches per day from December 1, 2025 to March 31, 2026.

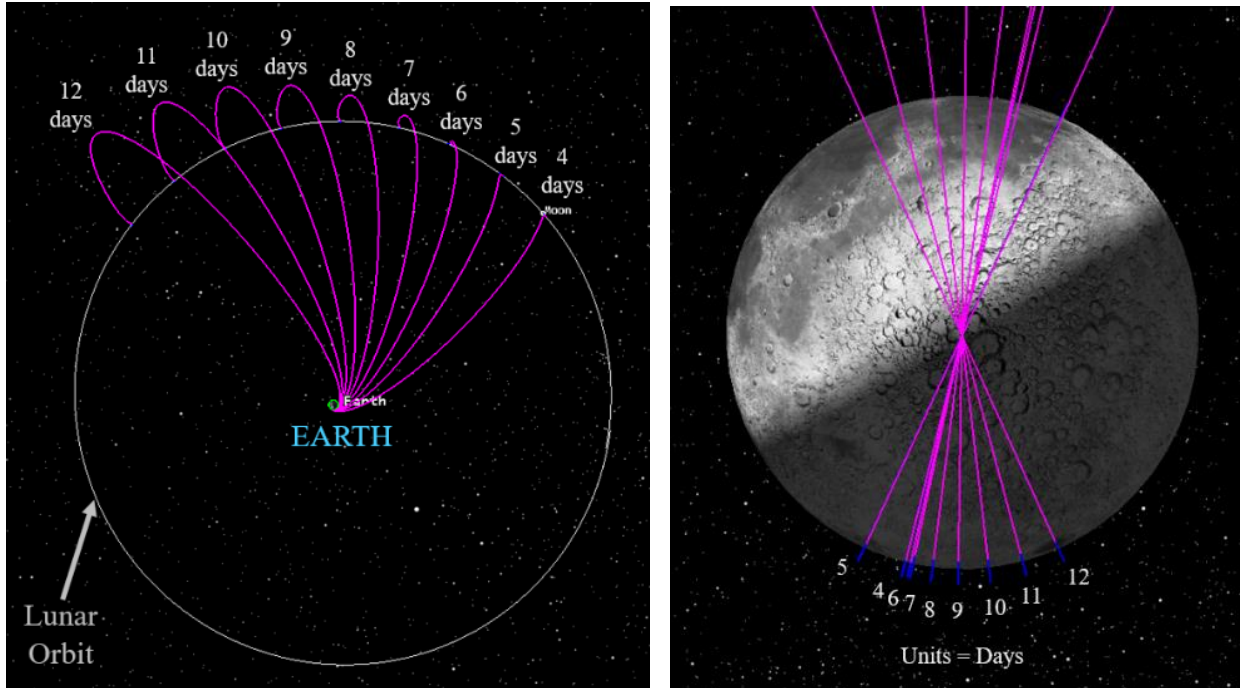


Fig. 14. TLI to LOI transit duration range from 4 to 12 days on same launch day (24-hour span) shown in ECI frame (left) and Moon-Sun rotating frame (right).

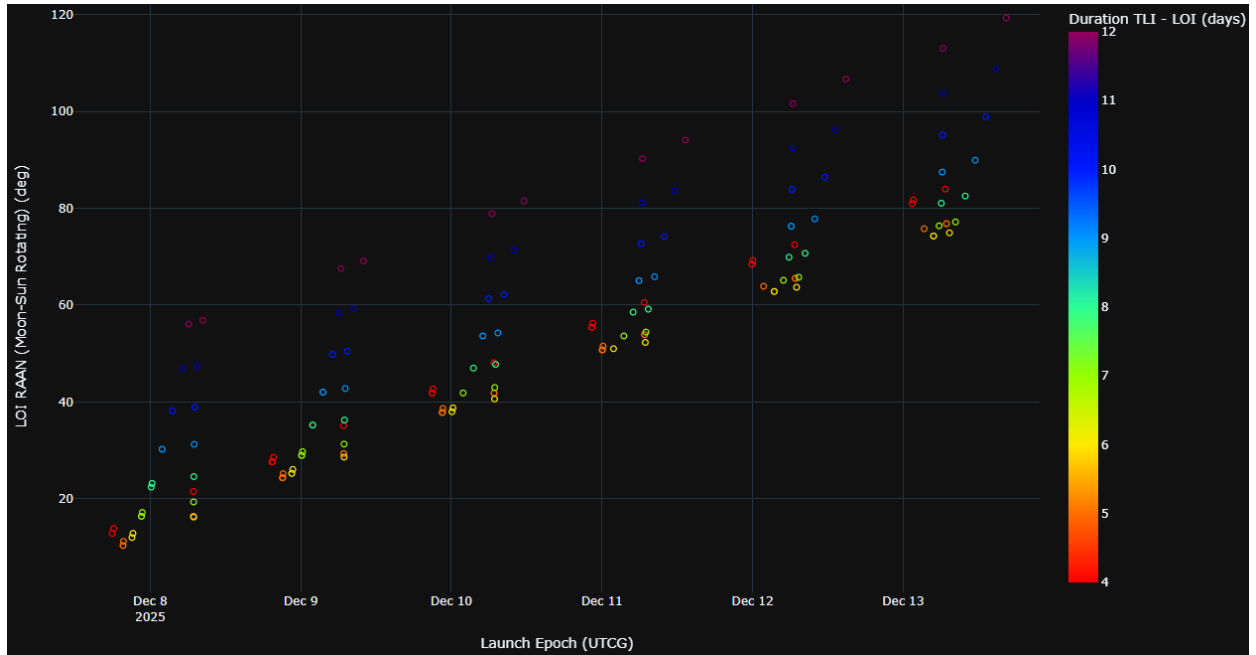


Fig. 15. TLI to LOI transit duration range from 4 to 12 days from December 7-13, 2025 showing RAAN(Moon-Sun) range of ~50 degrees possible every ~24 hours.

The ΔV cost of the LOI varies depending on the launch epoch and outbound transit duration as seen in Fig. 16. Specifically, the lowest LOI ΔV of ~797 m/s is yielded from the 5-day outbound transit duration, while the maximum LOI ΔV ~980 m/s for the 12-day duration.

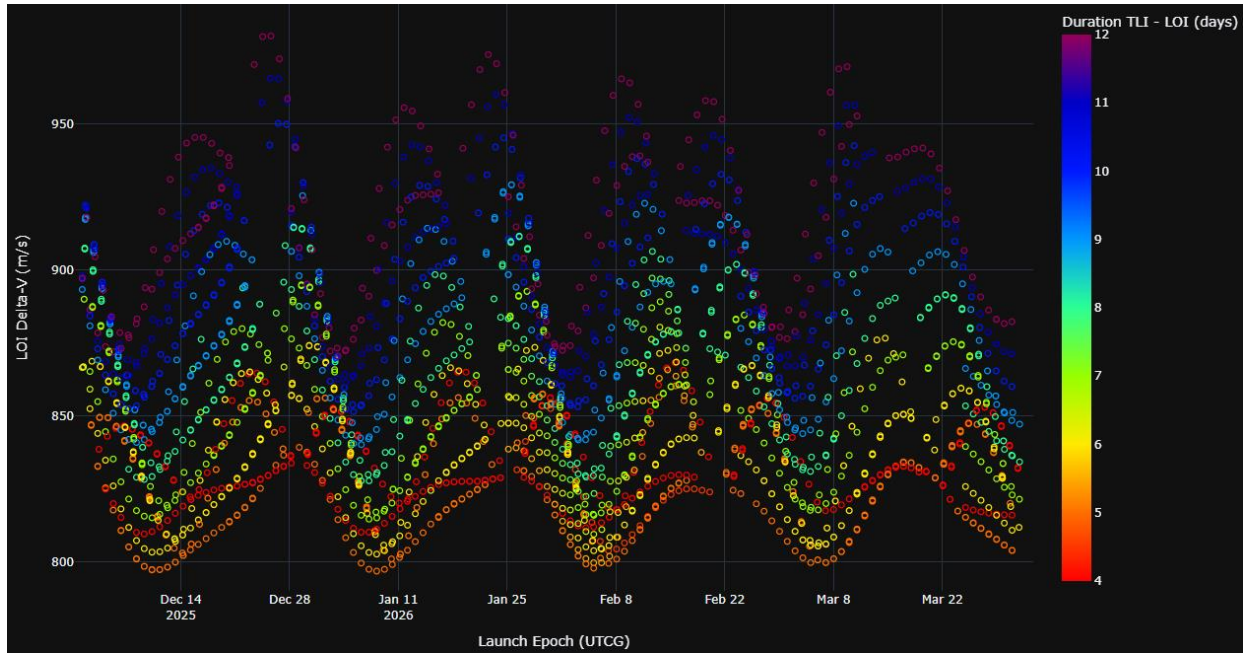


Fig. 16. LOI ΔV vs. Launch Epoch with outbound (i.e., TLI to LOI) transit duration range from 4 to 12 days, plotted from December 1, 2025 to March 31, 2026.

The direct trajectories seen in Figs. 14 and 15 were then modified to target *HELOs* which have similar properties to NRHOs and similar applications to concepts using alternate phased NRHOs (i.e., flexibility in approach angle upon landing and increased mission opportunities for *Artemis III*).

The presented *HELOs* contain an initial perilune that is allowed to vary such that the subsequent perilune altitude matched that of the baseline NRHO (~1,500 km). The LOI ΔV was delayed to ~2 hours after perilune to achieve the apsides requirement of the baseline NRHO (~90 degrees). Finally, the magnitude of the LOI ΔV was selected such that the orbit period of the *HELO* approximately matched the mean period of the baseline NRHO (~6.5 days). Although this result is achieved immediately after the LOI, a lower orbit period of ~5 days is yielded at the following perilune. The apolune altitude of these *HELOs* varied from ~55,500 to ~58,600 km as measured at the apolune following LOI.

The resulting *HELOs*, with transfer duration from TLI to LOI varying between 4 and 12 days, are seen in both the Moon-Earth and Moon-Sun rotating reference frames in Fig. 17. The LOI ΔV needed to achieve these *HELOs* varied between 355.6 m/s and 432.2 m/s with a corresponding $RAAN_{Moon-Sun}$ range of ~71 degrees.

To assess orbit stability of the set of *HELOs* seen in Fig. 17, these trajectories were propagated for one year. While these orbits were not optimized for stability, none of the cases yield an escape from the Moon's vicinity (or passage below 100 km lunar orbit altitude) for at least 100 days. The propagated orbits can be seen in both the Earth-centered inertial reference frame (Fig. 18, left) and Moon-Earth rotating reference frame (Fig. 18, right).

Future work can be performed on the presented *HELOs* and related orbits to investigate orbit symmetry, stability, and construction of crewed return opportunities back to Earth.

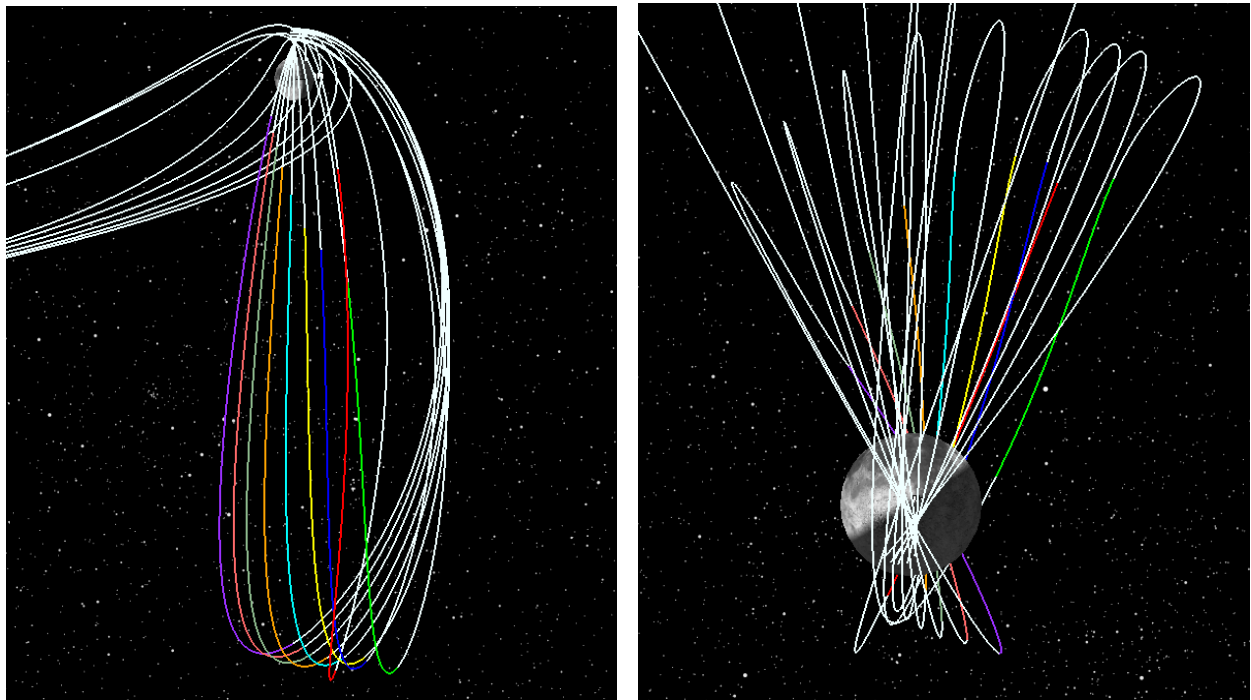


Fig. 17. Highly Elliptical Lunar Orbits, with similar properties NRHOs, have outbound (i.e., TLI to LOI) transit duration varied from 4 to 12 days, with resulting trajectories displayed in the Moon-Earth rotating reference frame (left) and from above the lunar north pole in the Moon-Sun rotating reference frame (right).

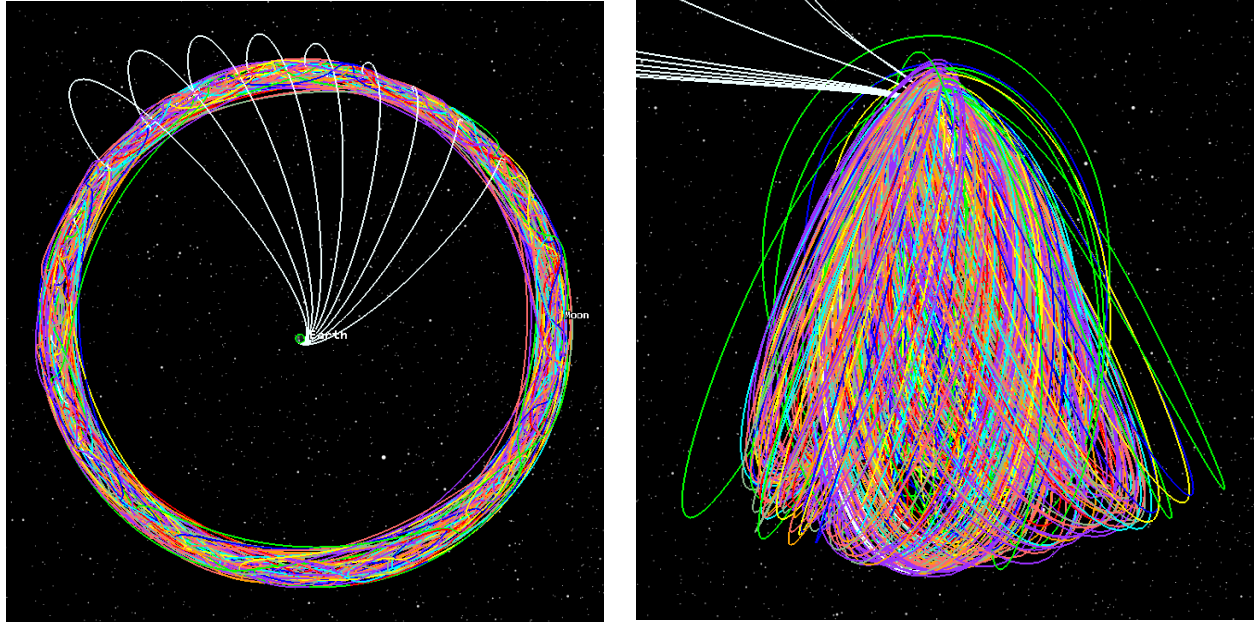


Fig. 18. Highly Elliptical Lunar Orbits, with similar properties to NRHOs, have outbound (i.e., TLI to LOI) transit duration varied from 4 to 12 days, displayed in the Earth-centered inertial reference frame (left) and Moon-Earth rotating reference frame (right) after one year of propagation.

B. Low Lunar Stable Orbit

A search for a lunar frozen orbit near the *HLS* pre-descent LLO was performed to serve applications such as a location for storage (e.g., propellant or crew supplies for program sustainability), a safe-haven orbit for rescue and other contingency scenarios, disposal and planetary protection (e.g., lunar graveyard orbits; planetary sample holding location), and/or communications relay orbit between the lunar surface and lunar orbit. The semi-major axis, a , of the studied orbit was modified to fit between values published by Lara [12] and above that shown by Folta & Quinn [13]. The specific semi-major axis value assumed was 1,913 km, with argument of perilune set to 90 degrees.

What then followed was an eccentricity scan within STK/Astrogator to determine the value of e that yielded the most stable orbit. It is seen in Fig. 19 that over a 1-year propagation duration with initial epoch of Dec. 2024, e and ω are bounded in the smallest region of the polar plot when $e = 0.022$. Note that the true anomaly, ν , of the orbit is assumed to be 0 degrees for all cases. Thus, for the selected low lunar frozen polar orbit: $[a, e, i, \omega, \nu] = [1,913 \text{ km}, 0.022, 90 \text{ deg}, 0 \text{ deg}]$.

Then, over a propagation period of 10 years, a *RAAN* scan in the MCI frame was performed for the selected low lunar frozen polar orbit. It is seen in Fig. 20 that for the full 360-degree range of nodes (assuming increments of 30-degrees), all orbits are stable with the perilune altitude notably remaining above ~110 km for all cases.

Of note is that to transfer to (or from) the selected low lunar frozen polar orbit from (or to) a nearby 100 km polar circular orbit, less than 33 m/s of ΔV is required. Given the perilune altitude of the presented lunar frozen polar orbit is near 120 km, even less ΔV is required to transfer to or from a 120 km polar circular orbit, specifically $\Delta V < 24 \text{ m/s}$.

ECCENTRICITY SCAN

Polar Plot: (e , ω)

$a=1913\text{km}$,

$\text{ecc}: [0.012, 0.032]$

$a_{1913\text{km}}_i_{90_e_{0p012_1\text{yr}}}$ - Argument_of_Perilune (deg)
 $a_{1913\text{km}}_i_{90_e_{0p016_1\text{yr}}}$ - Argument_of_Perilune (deg)
 $a_{1913\text{km}}_i_{90_e_{0p020_1\text{yr}}}$ - Argument_of_Perilune (deg)
 $a_{1913\text{km}}_i_{90_e_{0p022_1\text{yr}}}$ - Argument_of_Perilune (deg)
 $a_{1913\text{km}}_i_{90_e_{0p024_1\text{yr}}}$ - Argument_of_Perilune (deg)
 $a_{1913\text{km}}_i_{90_e_{0p028_1\text{yr}}}$ - Argument_of_Perilune (deg)
 $a_{1913\text{km}}_i_{90_e_{0p032_1\text{yr}}}$ - Argument_of_Perilune (deg)

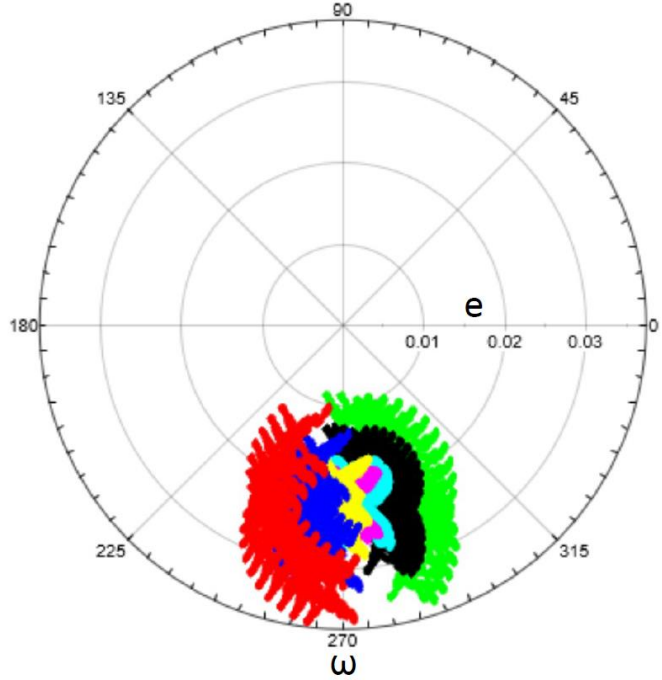


Fig. 19. Eccentricity scan with e and ω displayed on polar plot assuming 1-year of propagation duration for fixed value of $a = 1,913$ km and $i=90$ deg.

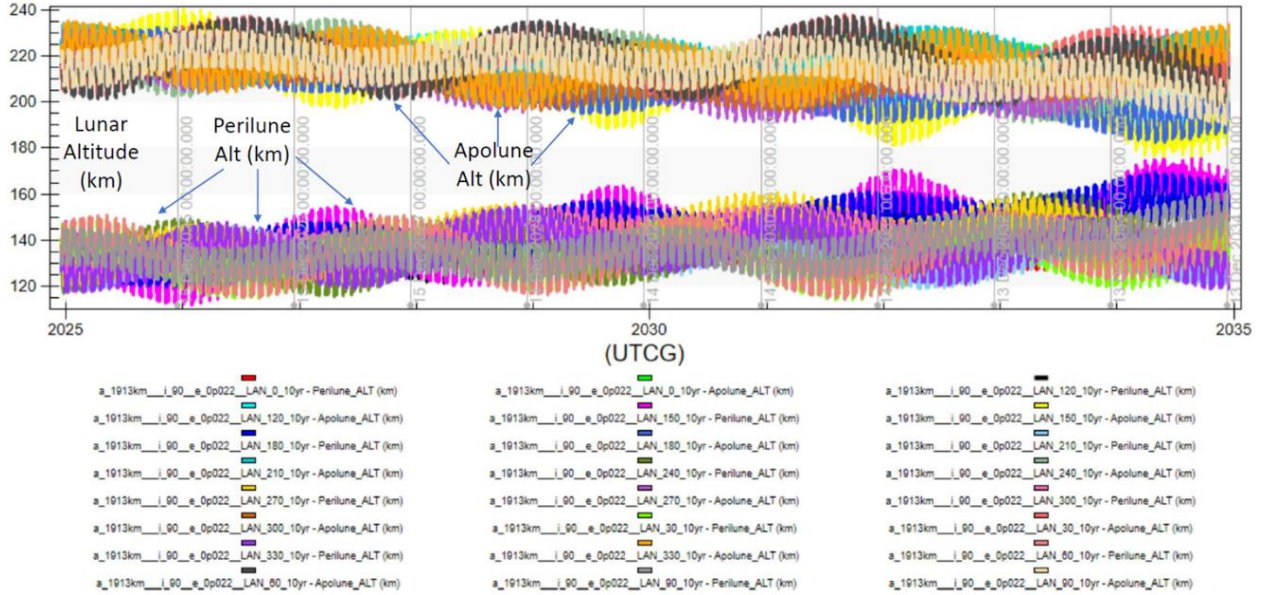


Fig. 20. Perilune and Apolune Altitudes plotted for frozen polar LLO vs. Time over 10-year Propagation period for 360-deg range of RAAN (MCI frame) in 30-degree increments with initial epoch in Dec. 2024 and: $[a, e, i, \omega, v] = [1,913 \text{ km}, 0.022, 90 \text{ deg}, 0 \text{ deg}]$.

Given *Artemis III* crew landing sites may be located ~ 5 degrees from the south pole [14], the corresponding inclination range of transfers from NRHO was calculated as 85 to 93 degrees. Thus, the lunar orbit studied in the previous polar case, with $a = 1,913$ km, $e = 0.022$, (i.e., 95X206 km perilune and apolune altitude dimensions), and $\omega = 90$ degrees was targeted from NRHO with insertion on Dec. 24, 2024. The MCS targets perilune from NRHO as 206 km (i.e., the apolune altitude of the final lunar orbit) followed by a circularization maneuver such that the line of

apsides can be selected to align with the lunar polar axis to ensure $\omega = 90$ degrees via the final maneuver which also lowers the perilune altitude to the required 95 km of the final orbit.

Nine cases were considered with lunar inclination varying from 85 to 93 degrees, in 1-degree increments. It was observed that all nine cases exhibited stable behavior, with most cases yielding circulating stable orbits over a 10-year propagation period as seen in Fig. 21. The perilune altitude of all nine cases were plotted over time with the results seen in Fig. 22; all trajectories remain above ~ 76 km over this 10-year period (the lowest perilune altitude is yielded by the 85-degree inclination case). Finally, the lunar inclination evolution in the Moon true-of-date (TOD) reference frame is plotted vs. time throughout the 10-year propagation period (Fig. 23). Future work will expand this trade space.

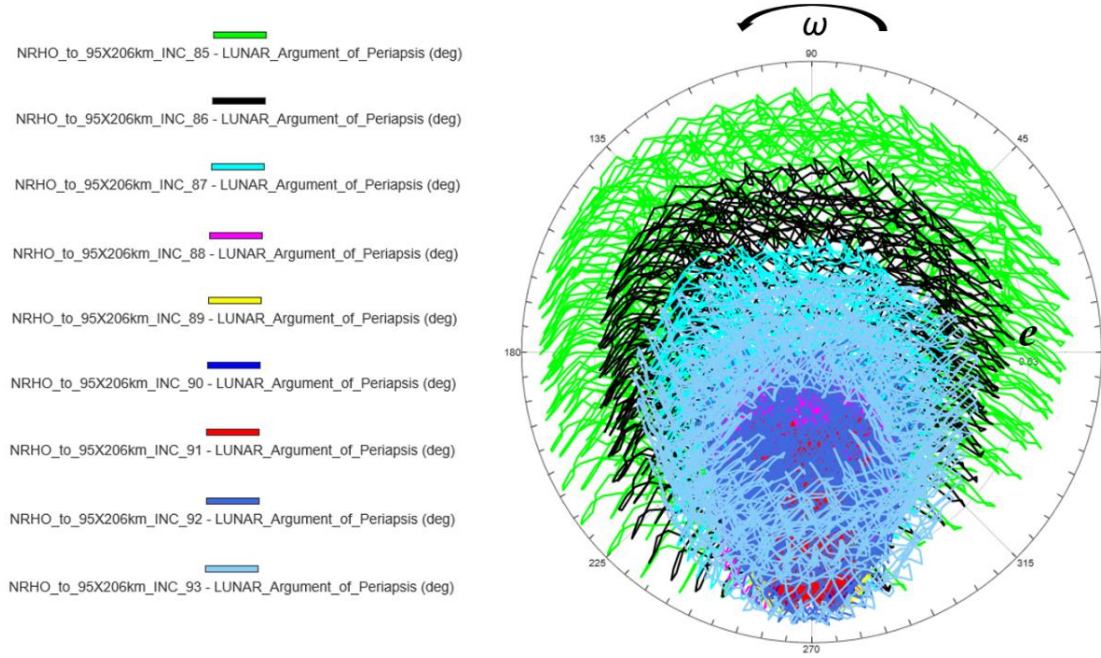


Fig. 21. Inclination scan from $i = 85$ to 93 degrees in 1-degree increments for 95X206 km with e and ω displayed on polar plot with 10 years of propagation duration assuming transfer from NRHO.

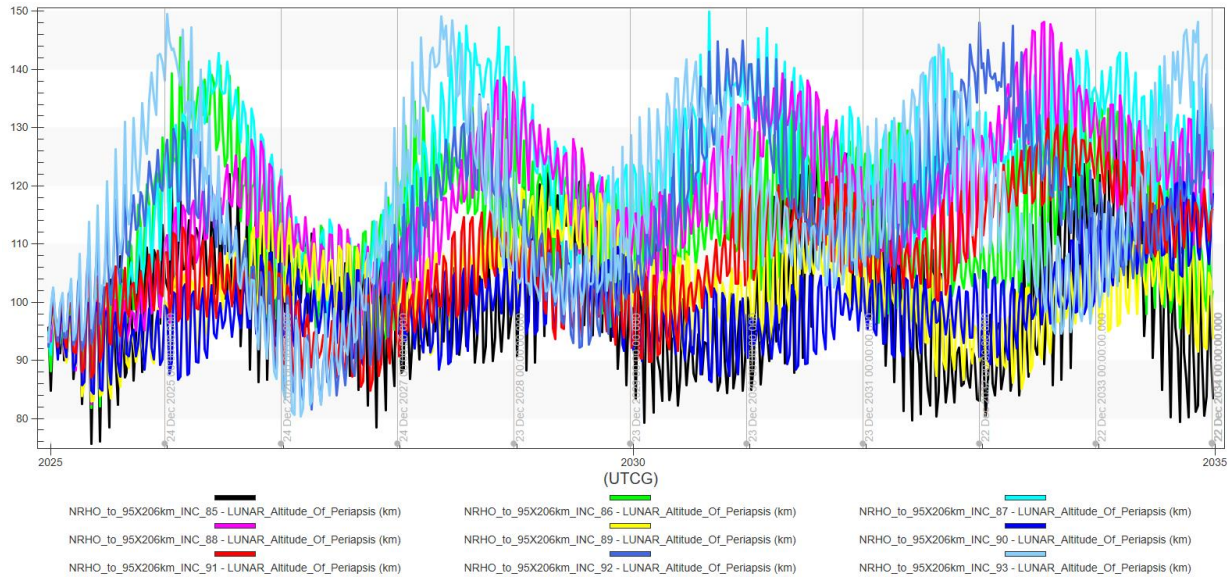


Fig. 22. Perilune Altitudes plotted for 95X206 km lunar orbit vs. Time over 10-year Propagation period for inclination range of 85 to 93 degrees in 1-degree increments with initial epoch on Dec. 24, 2024 assuming transfer from NRHO.

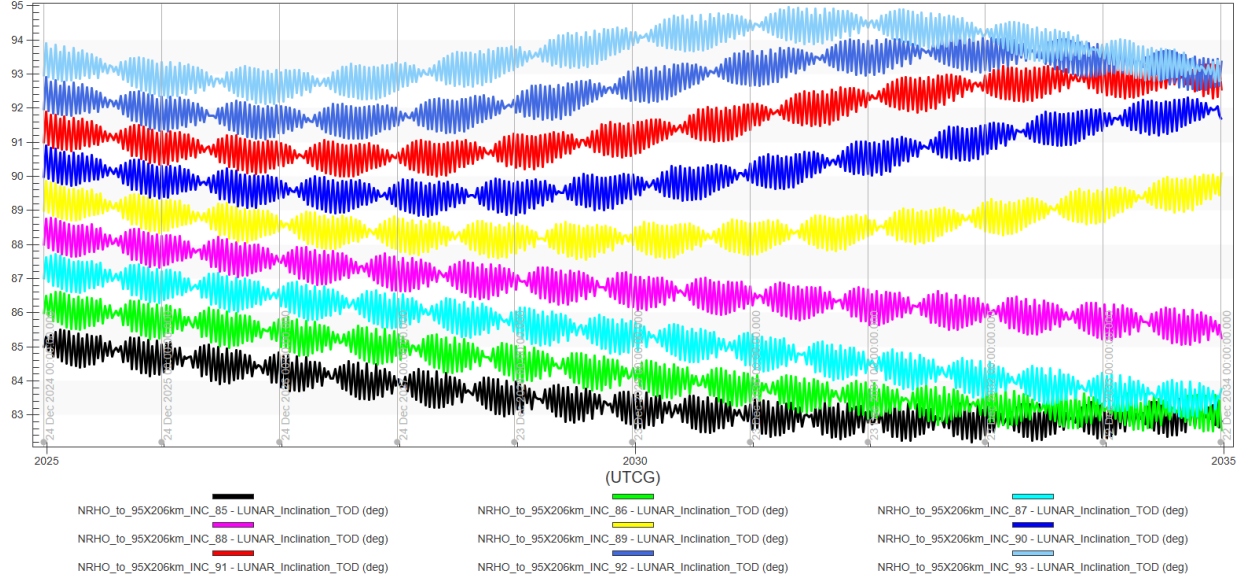


Fig. 23. Inclination plotted for 95X206 km lunar orbit in the Moon TOD frame vs. Time over 10-year Propagation period for inclination range of 85 to 93 degrees in 1-degree increments with initial epoch on Dec. 24, 2024 assuming transfer from NRHO.

VII. Conclusion

Preliminary trajectory analysis has been performed from TLI to lunar polar orbit using the *Lunar Browser* tool which is still evolving in a developmental phase. Modifications and extensions of these foundational trajectories were then applied to both NASA's *CLPS* and *Artemis* programs.

The $RAAN_{Moon-Sun}$ at LOI was shown to be a critical parameter in determining lighting conditions for landing sequences emanating from lunar polar orbit. Notably, in the section applying to NASA's *CLPS* program, in particular to the *CS-3* mission, it was found that $RAAN_{Moon-Sun}$ values of **~120, ~270, and ~300 degrees** (measured at LOI from the *Lunar Browser* results) yield lunar landings shortly after dawn at a specified farside site. Of note is that $RAAN_{Moon-Sun}$ ~270 and ~300 degrees yield relatively low loiter duration requirements (i.e., ~7 days) in LLO assuming a relay satellite is dropped off in ELFO with posigrade and retrograde orbital inclinations, respectively. However, of the latter two solution families, the retrograde southeast family yields ~5 times more cumulative hours of relay to surface contact duration throughout the daylight hours following landing given the location of the ELFO's apolune on the lunar farside. Thus, the retrograde southeast solution family is considered the most favorable family and was explored in more detail to show solutions through January of 2027 with time spent in various flight phases plotted vs. launch epoch. Additionally, the ELFOs for the retrograde southeast family displayed in Table 2 (i.e., Trajectories #1, #5, and #9) were propagated, with the corresponding perilune altitude plotted over time, to show that these ELFOs are stable for at least 5 years. Future work will analyze long-term propagation for an expanded solution set that includes all families.

Within the NASA *Artemis* program application section, it was stated that flexibility with the $RAAN_{Moon-Sun}$ at LOI yields flexibility with regard to approach angle upon descent and landing on the lunar surface which could expand mission opportunities (e.g., for *Artemis III*). This application would be achieved by substituting an alternate phased NRHO or HELO for the baseline NRHO. It was shown that if a launch can occur on any day of a month, then a 360-degree range of $RAAN_{Moon-Sun}$ can be realized upon landing when considering only the cases when the LOI is performed above the north pole of the Moon. For a fixed launch period of ~24 hours, the possible range of $RAAN_{Moon-Sun}$ is ~71 degrees if the outbound transit duration from TLI to LOI can be varied from 4 to 12 days assuming use of a HELO, which contained a corresponding LOI ΔV range from 355.6 to 432.2 m/s. The set of *HELOs* were propagated for one year to assess orbit stability, with all cases remaining in the Moon's vicinity for at least 100 days. Future work can focus on the presented *HELOs* and related orbits and investigate orbit symmetry, stability, and construction of crewed return opportunities back to Earth.

Finally, the stability of low lunar orbits with an inclination range between 85 and 93 degrees was presented, given these inclination values represent bounding cases for landing sites considered by the *Artemis* program. All presented LLOs exhibited stable behavior over a 10-year propagation period with the minimum perilune altitude of ~76 km resulting from the 85-degree inclination case. Future work will involve long-term propagation of the presented LLOs and proximate stable orbits over a 360-degree range of *RAAN*.

Acknowledgments

The authors are appreciative of the support received across multiple NASA centers and programs including: NASA Ames Research Center Spaceflight Division (notably Dr. Sally Cahill, David Mauro, and Andres Dono Perez), NASA *CLPS* program (notably Dr. Regina Blue, Chris Culbert, and Dr. Ahmed Fadl), and the NASA *Artemis* program (specifically *HLS* and notably Dr. Gregory Dukeman, Ruth Conrad, and Sonya Dillard).

References

- [1] *Commercial Lunar Payload Services Overview* [online resource]. URL: <https://www.nasa.gov/commercial-lunar-payload-services-overview> [retrieved May 10, 2023].
- [2] *Artemis* [online resource]. URL: <https://www.nasa.gov/specials/artemis/>, [retrieved May 10, 2023].
- [3] *Humans on the Moon, "About Human Landing System Development"*, [online article]. URL: <https://www.nasa.gov/content/about-human-landing-systems-development> [retrieved May 10, 2023].
- [4] NASA Selects Blue Origin as Second Artemis Lunar Lander Provider, *NASA*, [online article]. URL: <https://www.nasa.gov/press-release/nasa-selects-blue-origin-as-second-artemis-lunar-lander-provider>, [retrieved May 19, 2023].
- [5] National Cislunar Strategy for Science & Technology Policy, White House Office of Science & Technology, Nov. 2022
- [6] NASA Picks Firefly Aerospace for Robotic Delivery to Far Side of Moon, (March 14, 2023), [online article]. URL: <https://www.nasa.gov/press-release/nasa-picks-firefly-aerospace-for-robotic-delivery-to-far-side-of-moon>, [retrieved May 10, 2023].
- [7] NASA Payloads for (CLPS Science) CS-3 – TBD, [online resource]. URL: <https://science.nasa.gov/lunar-discovery/deliveries/cs-3>, [retrieved May 10, 2023].
- [8] Ely, T. A., "Stable Constellations of Frozen Elliptical Inclined Lunar Orbits," *Journal of Astronautical Sciences*, Vol. 53, No. 3, July-September 2005, pp. 301-316.
- [9] Artemis III: NASA's First Human Mission to the Lunar South Pole (January 13, 2023), [online article]. URL: <https://www.nasa.gov/feature/artemis-iii>, [retrieved May 10, 2023].
- [10] NASA FY24 Budget Request (March 7, 2023), [online resource]. URL: https://www.nasa.gov/sites/default/files/atoms/files/fiscal_year_2024_nasa_budget_summary.pdf [retrieved May 11, 2023].
- [11] Burke, L., Genova, A., Mahanjan, B., & Qu, M., "Analysis of the Approach Direction of the Human Landing System to a South Pole Landing Site Subject to Lighting and Communication Constraints," *AAS/AIAA Astrodynamics Specialist Conf.*, Charlotte, NC, Aug. 7-12, 2022.
- [12] Lara, M., "Design of long-lifetime lunar orbits: A hybrid approach," *Acta Astronautica* **69** (2011) 186-199.
- [13] Folta, D., & Quinn, D., "Lunar Frozen Orbits," *AIAA/AAS Astrodynamics Specialist Conference and Exhibit*, Keystone, CO, August 21-24, 2006.
- [14] Moon to Mars, "NASA Identifies Candidate Regions for Landing Next Americans on the Moon", (August 19, 2022), [online press release]. URL: <https://www.nasa.gov/press-release/nasa-identifies-candidate-regions-for-landing-next-americans-on-moon>, [retrieved May 11, 2023].